energies

MDPI

Article

Effects of Fracture Parameters on VAPEX Performance: A Numerical and Experimental Approach Utilizing Reservoir-On-The-Chip

Aria Rahimbakhsh and Farshid Torabi *

Petroleum Systems Engineering, Faculty of Engineering and Applied Science, University of Regina, Regina, SK S4S0A2, Canada
* Correspondence: farshid.torabi@uregina.ca; Tel.: +1-306-585-5667

Abstract: The present research carries out an in-detail study of the VAPEX process as one of the most recent solvent-based heavy oil recovery techniques in fractured reservoirs to evaluate the effect of fracture parameters on process performance. To achieve this purpose, several fractured patterns with distinct features were designed and engraved on glass pieces to manufacture state-of-the-art microfluidic models mimicking a typical Canadian heavy oil reservoir. A heavy oil sample of viscosity 1514 cP was utilized during the conducted experiments with pure propane and pure carbon dioxide as the injection solvents. A thorough image analysis operation was carried out over the experimental models to determine heavy oil produced, residual oil saturation, ultimate recovery factors, and monitor solvent chamber expansion. Numerical simulations of the same experiments were carried out for history matching and predicting other designed scenarios. Error analysis revealed average absolute errors of below 8%, showing convincing precision. Together with the simulation outcomes, a comprehensive data bank was obtained from the 30 scenarios designed and 18 VAPEX experiments conducted. The effects of fracture orientation, length, width, intensity, and position on process performance were identified and numerically evaluated. It was observed that all fractures, regardless of their properties, enhanced heavy oil recovery in comparison to the base case (no fractures) scenario. Moreover, propane proved more efficient owing primarily to its higher solubility and effective dispersion. The highest recovery factor, 65.81%, was obtained when implementing two wide vertical fractures on either side of the well pair. Almost equal to that, 64.93% was the process efficiency by positioning two long horizontal fractures between the wells.

Keywords: VAPEX; fractured reservoir; recovery factor; microfluidic model; image analysis

Citation: Rahimbakhsh, A.; Torabi, F. Effects of Fracture Parameters on VAPEX Performance: A Numerical and Experimental Approach Utilizing Reservoir-On-The-Chip. *Energies* **2023**, *16*, 1460. https://doi.org/10.3390/en16031460

Academic Editor: Md. Imran Hossen Khan

Received: 3 January 2023
Revised: 27 January 2023
Accepted: 31 January 2023
Published: 2 February 2023

1. Introduction

Numerous heavy oil and bitumen reservoirs exist around the world. Regarding ever-growing energy demands, economic aspects, and rising environmental concerns, these underground resources need to be produced via advanced, environmentally friendly, and economically viable methods. Implementation of such techniques can secure the future of the heavy oil industry.

To overcome the deficiencies inherent to thermal-based techniques, such as excessive energy consumption and heat loss, solvent-based methods were developed, which enabled viscosity of heavy oil to be diminished by dissolving a solvent in the bulk phase of the target zone. Indeed, they seemed to reduce energy consumption, related production costs (for minimal surface facilities), and environmental effects while increasing the grade of obtained oil [1–4]. By switching from a thermal to a solvent-based technique, the requirement to utilize massive amounts of water and, therefore, emit damaging greenhouse gases is eliminated, resulting in an ecologically benign operation. Moreover, dissolving adequate solvent in the reservoir promotes asphaltene precipitation and, therefore, in situ upgrading of the heavy crude [5].

Vapour-assisted petroleum extraction (VAPEX) has been primarily used in oil sands reservoirs. A solvent vapour chamber is created, which extends sideways into the formation, raising the reservoir pressure. The solvent–oil interface enables solvent diffusion into undisturbed heavy oil, diminishing its viscosity. Under the influence of gravity, the diluted oil pours down the interface toward the horizontal production well that is completed at the reservoir's bottom [6].

Equilibrium pressure, molecular weights of the formation fluid and gaseous solvent, and associated density difference between the fluids, solubility, diffusion coefficient, and subsurface conditions highlight the importance of solvent selection [7]. In particular, delivering a light vaporized solvent into a formation around its dew point ensures that solubility increases to its highest level possible [2,7]. Butler and Jiang [8] compared efficiency of propane and butane experimentally, which revealed the former as superior. In similar studies, Kok [9] and Yildirim [10] reported the same observation when various heavy oil systems were utilized. Despite propane being the more popular solvent in the VAPEX process due to its high effective dispersion coefficient and higher process performance, researchers' interest has recently shifted to CO_2-based solvent for environmental and cost-related reasons [11,12]. Torabi et al. [13] concluded that adding CO_2 to an injection solvent during VAPEX can be deemed a feasible approach.

One may notice the importance and current situation of the typical and other types of unconventional oil and gas, such as shale gas, hydrate, etc. Gao et al. conducted a numerical simulation study on the influence of different fracture attitudes on shale gas transport and then analyzed the sensitivity of their proposed model [14]. Li et al. analyzed the rheological characteristics and reservoir damage of CO_2 fracturing fluid in low-permeability shale reservoirs. According to their results, a reference for CO_2 fracturing technology was obtained [15]. Li and Wu studied the factors affecting a safe mud weight window in hydrate-bearing formations in a Chinese reservoir. Accordingly, temperature, stress difference, and hydrate saturation were among the most influential parameters [16]. Finally, Chen et al. simulated flow behaviors of heavy oil and its asphaltic residues through horizontal pipes by employing a filtered two-fluid model to predict mesoscopic flow. Therein, they obtained the distribution of the time-averaged asphaltic residues, residue velocities, solids pressure, and granular temperature along the radial direction [17].

Diffusion is a critical parameter in VAPEX and has been studied by numerous researchers [18,19]. It is the primary molecular mechanism responsible for gas absorption and, subsequently, mixture viscosity decline [7]. Molecular diffusion begins with gas travelling the transition layer and then infiltrating it before diffusing into the heavy oil bulk phase [20]. However, when operating a VAPEX process, gravity drainage leads to solvent–heavy oil motion, and, subsequently, dispersion plays an integral role in drainage. Kapadia et al. [21] created a theoretical approach for determining the dispersion coefficient of C_4H_{10} in a Canadian heavy oil sample. It was discovered that solvent dispersion and HO viscosity showed strongly composition-dependent behavior. El-Haj et al. [22], after performing VAPEX tests utilizing Cold Lake heavy oil in various glass beads, proposed a model capable of predicting the C_4 dispersion coefficient and the solvent's mass fraction at the gas/oil interface. According to their calculations, the obtained dispersion coefficients appeared to be about one thousand times greater than diffusion coefficients at the molecular levels. Likewise, several studies have observed improved mass transfer [2,11,23–25].

Theoretical modeling of the VAPEX process has also attracted vast interest from scholars. Reservoir regions during the process were first classified by Butler and Mokrys [26] using a Hele-Shaw cell, which was followed by derivation of a drainage rate predictive model. Das and Butler [2] upgraded that for a porous medium. In an experimental attempt to evaluate impact of drainage height on heavy oil recovery and production rate during VAPEX, Yazdani and Maini [25] chose three distinct heights and obtained two valid correlations. Moghadam et al. [27] introduced an analytical model capable of describing rising and expansion of the chamber. Accordingly, Darcy's equation was combined with geometric formulas to obtain cumulative oil production. Ma et al. [28] proposed a parabolic

shape (both convex and concave) for solvent chamber edges. Their subsequent analytical model was derived through assuming a constant thickness for the interface wherein heavy oil saturation decreases instantly from S_{oi} to S_{or}.

However, there is a tangible lack of sufficient experimental and numerical studies on VAPEX performance in fractured reservoirs. Due to the large matrix and fracture permeabilities, the injected solvent is expected to spread through the latter prior to diffusing into the former. Meanwhile, fracture characteristics, such as length (which specifies how far solvents can reach into the reservoir), width, position (with respect to injection and production well pair), intensity, and inclination (horizontal and vertical) play a significant role in process efficiency [29]. In general, fractures' presence is deemed to enhance heavy oil production because of providing increased solvent–heavy oil contact as well as enhancing the main drainage mechanism, gravity drainage, especially by vertical fractures [30–34].

Most of the experimental studies have been conducted in sand-packed models, where, due to practical aspects of test preparations, crucial process parameters vary from one test to another. Porosity, permeability, and the porous medium structure are among those. This paper experimentally studies the VAPEX process in fractured reservoirs by employing state-of-the-art microfluidic models to keep reservoir physical properties constant between similar tests and obtain precise evaluation of each parameter's influence under pre-designed circumstances. Furthermore, clear-cut and real-time visualization of the process can be completed at each stage of injection production. Finally, a numerical simulation model was constructed and history-matched against the collected data to enable further analysis of recovery factors and fractures' effects.

2. Materials and Methods

The materials, apparatus, and measuring methods used in the experiments are briefly introduced below. First, the equipment and materials, such as heavy oil–solvent systems, pumps, laser machine etc., are introduced. Then, construction of the microfluidic models is explained in detail along with the required procedures. The next section introduces the pattern designs and rationale for selecting each one. After that, the experimental conditions at which the lab tests were carried out are described. This section is followed by an introduction to the image analysis technique, which was used for assessing the performance of each VAPEX test. Finally, construction of a reliable simulation model is discussed in detail along with the history matching procedures.

2.1. Materials and Equipment

A sample of Canadian heavy oil was obtained and characterized prior to conducting the experimental work. The viscosity, density, and molecular weight were measured at room temperature to be 1.514 N.s/m^2, 974.2 kg/m^3, and 374 kg/kmol, respectively. Pure propane and carbon dioxide were utilized as the injection solvents. 0.01 m thick clear glass was utilized for micromodels preparations. Transfer cylinders, pressure gauges, gas cylinders, vacuum pumps, LED light source, back pressure regulators, and various types of valves and connections were among the equipment used. Table 1 summarizes the main materials used for the laboratory tests. As suggested, a porosity of 100% was assigned to the fractures to highlight the channel-like structure with no grains inside.

Table 1. The reservoir and fluid properties.

Property	Value
Heavy oil viscosity at 20 °C	1.514 N.s/m^2
Heavy oil density at 20 °C	974.2 kg/m^3
Heavy oil molecular weight	374 kg/kmol
Injected solvents	Propane, carbon dioxide

Table 1. *Cont.*

Property	Value
Glass thickness	0.01 m
Glass length	0.2286 m
Glass width	0.127 m
Engraved pattern depth	6×10^{-4} m
Engraved pattern length	0.15 m
Engraved pattern width	0.043 m
porosity	35.2%
permeability	0.053 m^2
Initial reservoir pressure	790 kPa
Fracture porosity	100%
Fracture permeability	9.9 m^2

2.2. Microfluidic Models' Construction

One may note that this is possible only owing to the main privilege of using the microfluidic models: the formation remains the same from one experiment to another since the porous medium is indeed a fixed engraved pattern on a piece of glass. In contrast to experiments performed in sand-packed physical models, where maintaining crucial parameters such as porosity and permeability at desirable fixed values has remained an unresolved issue throughout the course of experiments, microfluidic models make that matter possible and enable the test operator to be in full charge of the tests. In other words, every discrepancy observed in the results of different experiments can readily be attributed to the change deliberately introduced to each scenario.

The microfluidic models employed in this thesis are composed of two pieces of glass of 0.01 m thickness fused into each other in a high-temperature furnace. To build one, first, AutoCAD was used to design a non-uniform porous medium pattern (Figure 1), and the resulting file was processed by LaserCAD so as to prepare it for being engraved by the laser machine, Boss Laser®, in the lab. With one engraved piece, a second intact piece of the same size was placed on it for both to remain in the furnace, heating them up to 690 °C to complete the model construction. The design of all microfluidic models, although featuring various fracture patterns and, therefore, being different, include 4 ports. The two ports on either end of the models enable access to the porous media for model saturation, permeability measurement, and cleaning purposes. The other two ports (i.e., the holes in the center of the models), as mentioned before, play the roles of injection/production wells. The top hole is used for delivering the injection fluid (gas solvents), while the bottom one is used for heavy oil and solvent production. Moreover, Table 1 includes the pattern dimensions engraved on the glass.

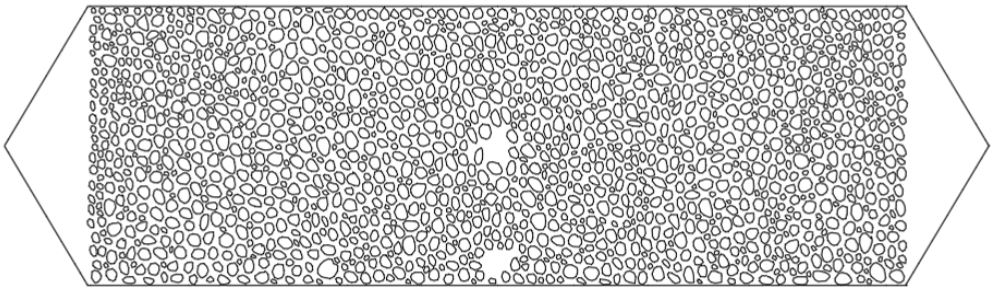

Figure 1. The design of a microfluidic model in AutoCAD.

2.3. Test Design

Calibrated digital gas flow meters (DFM) adjusted for each specific type of solvent were employed to control and record the solvent injection from the gas cylinders. A digital pressure gauge was mounted immediately on the injection production ports to register the associated pressures. Given the constant pressure approach to conducting the VAPEX experiments, the injection and production (BPR) pressures were fixed at 800 and 790 kPa, respectively. The pump was set at 790 kPa to maintain the outlet pressure of the microfluidic model through connecting to the top port of the BPR. Meanwhile, the side and bottom ports of the BPR were connected to the model outlet and fluids collection beaker, respectively.

The fracture designs encompass a variety of combinations of fracture parameters for each one to be accurately analyzed. As an instance, models with short and long fracture sizes were built and used for conducting actual tests. Then, in order to incorporate the effect of another parameter, say position, same-length fractures were designed at different locations within the pay zone. This strategy would allow for attributing the changes and recovery improvements to the parameter that was deliberately modified. This study considered the five fracture characteristics of length, width, inclination, intensity, and position. Including the conventional VAPEX test (no fractures), 15 patterns were designed and analyzed, as shown in Figure 2. Patterns with horizontal fractures were named H1 through H6, while those with vertical ones were named V1 through V8. These patterns were designed in a way to allow for all possible comparisons required.

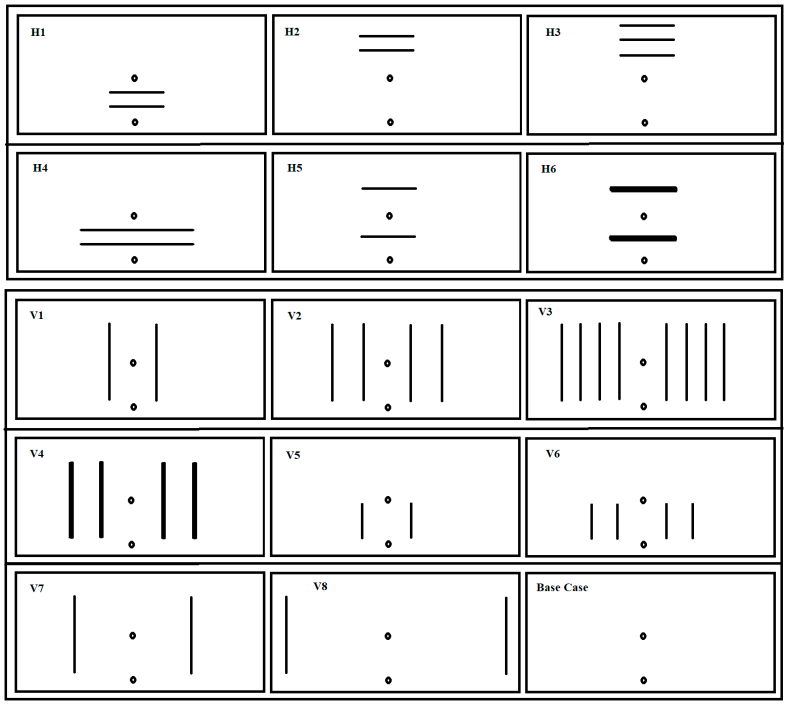

Figure 2. The fracture pattern designs.

Throughout the time of conducting experiments, several important parameters were monitored and recorded. A host computer was connected to specific data acquisition equipment with specific connection ports, converter parts, and pulse detectors. The digital gas flow meter (DFM), manufactured by AALBORG®, collected the data pertaining to time, gas flow rate, and instantaneous and total volumes injected and stored them as a file on the computer. Moreover, a Heise® digital pressure transducer made possible continuous recording of inlet and outlet pressures of the micromodels. Moreover, a high-resolution camera was placed in front of the microfluidic model to capture real-time images of the ongoing process. The pictures were later utilized for image analysis and recovery calculation purposes. In addition, to ensure better visualization of the glass microfluidic

system, a multi-setting LED light source was placed behind the models to improve the image capturing quality. Figure 3 illustrates the schematic design of the lab experiments.

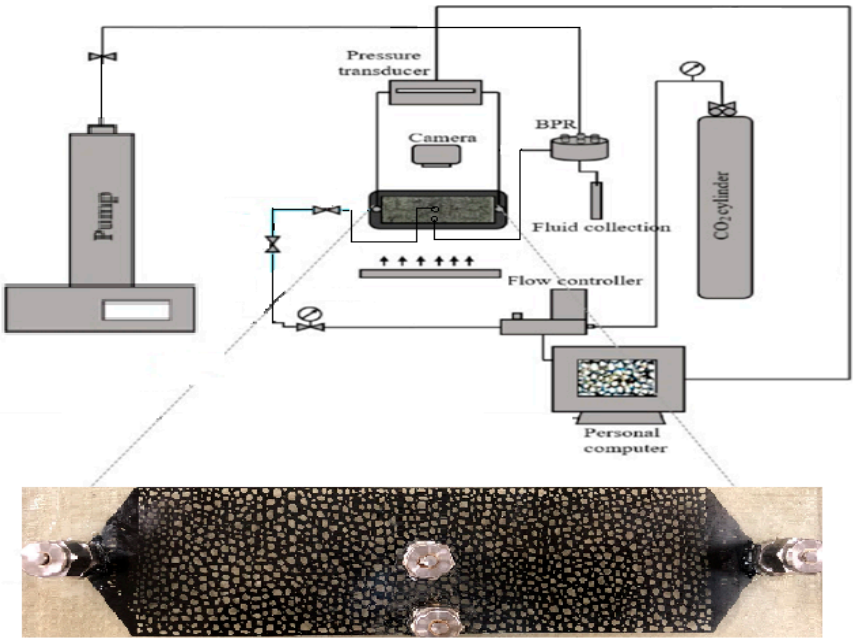

Figure 3. The design of a microfluidic model in AutoCAD.

2.4. VAPEX Tests

In the present study, 18 VAPEX tests were conducted in the lab using a typical Canadian heavy oil sample and two gas solvents in microfluidic models with distinct fracture designs. The solvents were introduced into the saturated models through the top access point in the middle (injector), while the bottom port served as the producer. A DFM was employed to conduct the injection fluid at a specific fixed pressure while recording the flow rate with respect to time throughout the process. Therefore, solvent injection rates and cumulative injection volumes were readily available for future analysis. At the same time, the BPR was connected to the producer to maintain a constant pressure slightly below that of injection.

A high-resolution camera was set in front of the model backed by LED lights to take numerous real-time images during the entire process, which were later used for image analysis (IA) purposes to evaluate heavy oil recovery as well as sweep efficiency. This would make possible clear-cut visualization of solvent chamber growth under different circumstances.

Conducting each VAPEX test took about 6–7 h depending on the heavy oil–solvent systems and experiment circumstances and demanded the physical presence of the operator to monitor and collect the data. The VAPEX process is a slow one in nature due to the main production mechanism (gravity drainage) relying on solvent diffusion and subsequent chamber propagation. According to the observations, the injection rate experienced an overall increasing trend with time and reached its highest at the end of the process. At that time, the solvent chamber ceased to spread considerably further (falling phase) and the injection gas tended to exit the model without significantly contributing to heavy oil production. Finally, injection was stopped and the corresponding valves were closed while releasing the production port to atmospheric pressure to collect any final production.

2.5. Image Analysis (IA) and Sweep Efficiency Measurement

This step began with solvent injection commencement and was carried out continuously during the whole process span. High-quality images were captured throughout the course of each VAPEX test to be employed for various purposes post-experiments. First, and most importantly, IA helped determine the precise value of recovery factor at each time step by analyzing the colors of each pixel and, hence, calculating the oil/solvent content

within that pixel. This was completed by primarily introducing the black heavy oil color as 100% oil saturation and the light yellow of the injection solvent as 100% solvent saturation zones. The obtained data points were later utilized in recovery comparisons between the various scenarios considered. A MATLAB® code was used to perform the image analysis operations, as illustrated in Figure 4. Figure 5, on the other hand, demonstrates the results of IA obtained for the base case VAPEX with carbon dioxide versus pattern H1 (horizontal fractures included) with propane injection.

```
he = imread("hestain.png");
imshow(he)
title("H&E Image")
text(size(he,2),size(he,1)+15, ...
     "Image courtesy of Alan Partin, Johns Hopkins University", ...
     FontSize=7,HorizontalAlignment="right")
numColors = 3;
L = imsegkmeans(he,numColors);
B = labeloverlay(he,L);
imshow(B)
title("Labeled Image RGB")
lab_he = rgb2lab(he);
ab = lab_he(:,:,2:3);
ab = im2single(ab);
pixel_labels = imsegkmeans(ab,numColors,NumAttempts=3);
B2 = labeloverlay(he,pixel_labels);
imshow(B2)
title("Labeled Image a*b*")
mask1 = pixel_labels == 1;
cluster1 = he.*uint8(mask1);
imshow(cluster1)
title("Objects in Cluster 1");
mask2 = pixel_labels == 2;
cluster2 = he.*uint8(mask2);
imshow(cluster2)
title("Objects in Cluster 2");
mask3 = pixel_labels == 3;
cluster3 = he.*uint8(mask3);
imshow(cluster3)
title("Objects in Cluster 3");
L = lab_he(:,:,1);
L_blue = L.*double(mask3);
L_blue = rescale(L_blue);
idx_light_blue = imbinarize(nonzeros(L_blue));
blue_idx = find(mask3);
mask_dark_blue = mask3;
mask_dark_blue(blue_idx(idx_light_blue)) = 0;

blue_nuclei = he.*uint8(mask_dark_blue);
imshow(blue_nuclei)
title("Blue Nuclei")
```

Figure 4. Image analysis code used for MATLAB®.

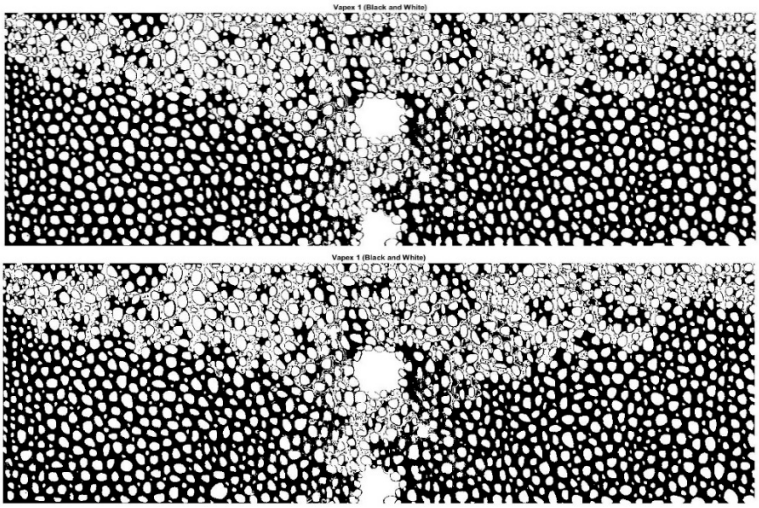

Figure 5. The IA analysis for conventional and a pattern with horizontal fractures.

Based on analysis of the IA, the sweep efficiencies were calculated for each set of heavy oil–solvent-fracture design. This was completed by finding the ratio of the area swept over the total area of the pattern.

2.6. Experimental Conditions

The VAPEX tests were conducted at room temperature. The initial reservoir pressure was set at 790 kPa, while the injection pressure was set slightly higher at 800 kPa. At the production end, the BPR, which was controlled by a pump, was maintained at 800 kPa as well to allow for non-pressure driven fluids production. Solvents were injected directly from gas cylinders through digital flow meters to record the injection rate as well as the cumulative gas injected. The injection rates varied in the range 0.01 to 0.05 cc/min during the experiments. One may note the pore volume of the models being about 1.7 cc, and, typically, 6–8 PV of solvent was injected in each test. Porosity and permeability measurements, model saturation with heavy oil, and model cleaning after each test were conducted in accordance with standard laboratory procedures. Furthermore, all equipment and chemicals were handled based on the relevant safe operations procedures (SOP).

2.7. Numerical Simulation

Heavy oil viscosity and density were measured at room temperature to construct a reliable set of PVT data. The Winprop^{TM} package in the CMG (Computer Modelling Group Ltd., Calgary, AB, Canada, 2020) software was employed to find the vapour pressures and phase envelopes of the solvents utilized in this study. Accordingly, vapour pressures of propane and carbon dioxide were determined to be 814.2 and 5597.9 kPa, respectively. Furthermore, solvents' solubilities in the heavy oil sample used in the present work were experimentally measured at various pressures, below their corresponding vapour pressures, and at room temperature. Figure 6 represents the solubility measurement results for both solvent–heavy oil systems.

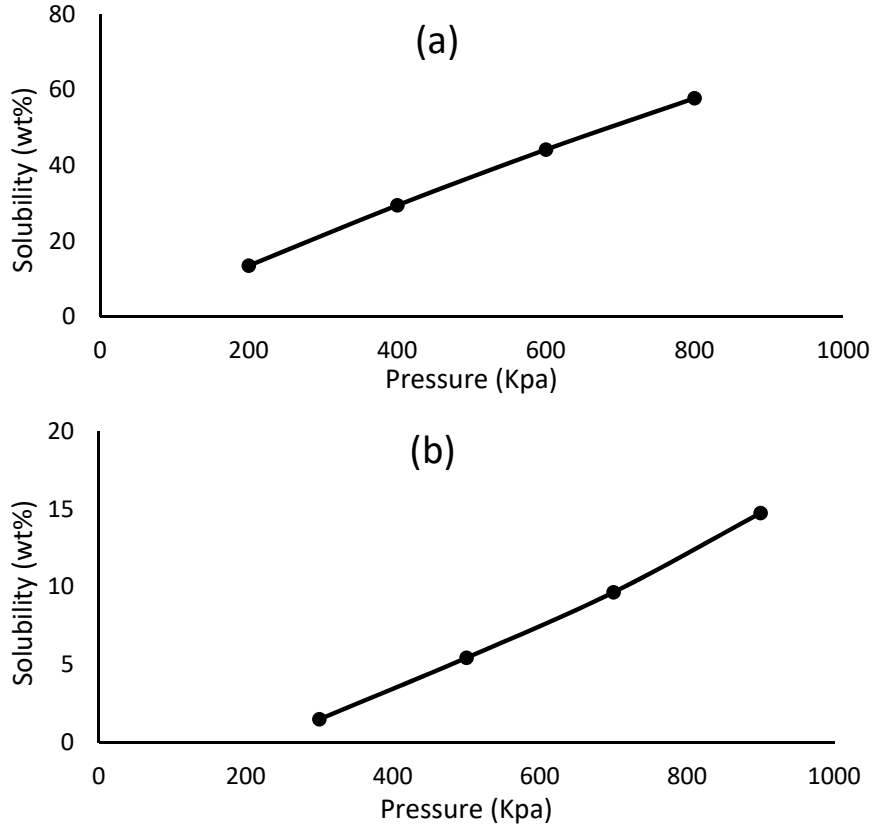

Figure 6. Solubility measurements of C_3 (**a**) and CO_2 (**b**) in the heavy oil sample.

The PVT set was developed by using the Winprop^{TM} package to adjust the parameters in the Peng–Robinson equation of state (EOS). This was accomplished by introducing the heavy oils carbon number distribution as the initial input to the package. Then, the heavy oil–solvent system main characteristics, such as density, viscosity, and solubility, were matched against the experimental data by tuning the EOS parameters. Once a best match was achieved, the constructed PVT unit was ready to be introduced to CMG STARS^{TM} to begin the VAPEX process simulations.

The reservoir patterns were then constructed in accordance with the 15 specified designs in the CMG STARS^{TM} software. Considering the number of solvent–heavy oil systems, a total of 30 VAPEX tests were designed. Given the constraints in time, materials, energy, and experimental workload, it was not possible to experimentally assess all VAPEX cases in the lab. Hence, the authors decided to first perform the history matching operation using the results collected from conducting the experimental VAPEX tests in 4 patterns (8 experiments) and, once complete, evaluate all 30 injection/production scenarios through simulation. It must be mentioned that 9 (including the four used for history matching) out of the 15 patterns were selected for experimental assessment of the VAPEX process, which still led to a convincing 18 lab tests.

After completing the simulation models, attempt was made to tune and match them against the experimental findings. To that end, the key input variables dispersion coefficient and relative permeability were selected for tuning. Several variations were tried out to obtain the closest match between the observed data and simulation outcomes. The base case (no fractures), H1, H4, and V1 were the four patterns utilized to achieve the best history matching. The corresponding average absolute errors remained below 8%, which shows an adequately precise history matching operation. Factors such as unsteady expansion of the solvent chamber during the short first phase of the VAPEX process, transition from single-phase to two-phase production, and the corresponding change in injection and production rates, non-uniform grain design on either side of the centralized well pair, and experimental human errors can be named as the error sources.

Figure 7 shows the reservoir constructed for pattern V2. As depicted in Figure 2, this pattern includes two vertically positioned fractures on either side of the injection production well pair. Figure 8 indicates the results of history matching for the base case scenario. It must be mentioned that, to obtain the optimum fracture dimensions and ensure their consistency in size with the microfluidic models in both experimental works and the designed simulation runs, several trials and errors were carried out first. The absolute errors associated with propane and carbon dioxide injection in this case were found to be 4.98% and 5.40%, respectively. In this figure, the recovery factors are demonstrated versus the equivalent pore volume of the liquid solvent injected.

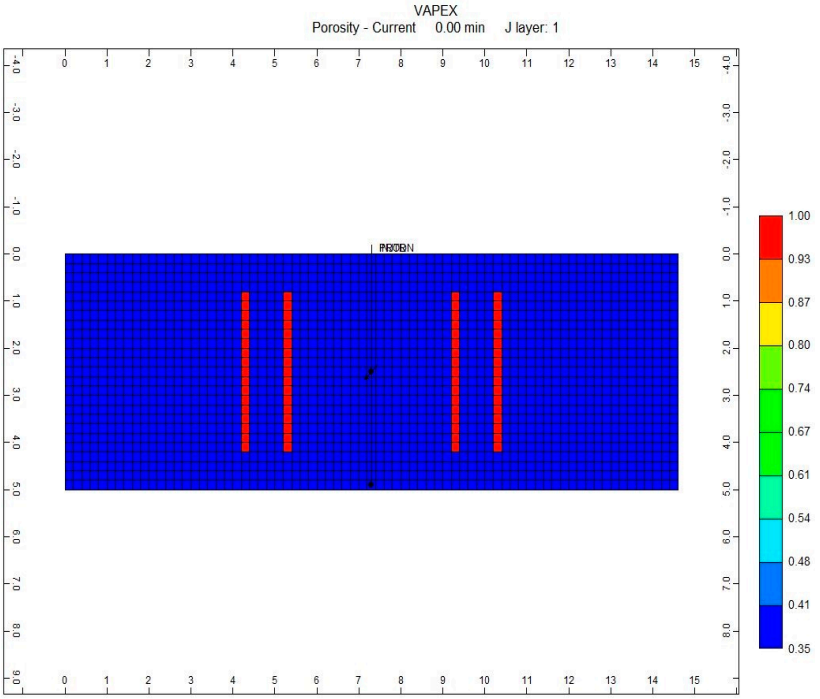

Figure 7. History matching results in the base case scenario.

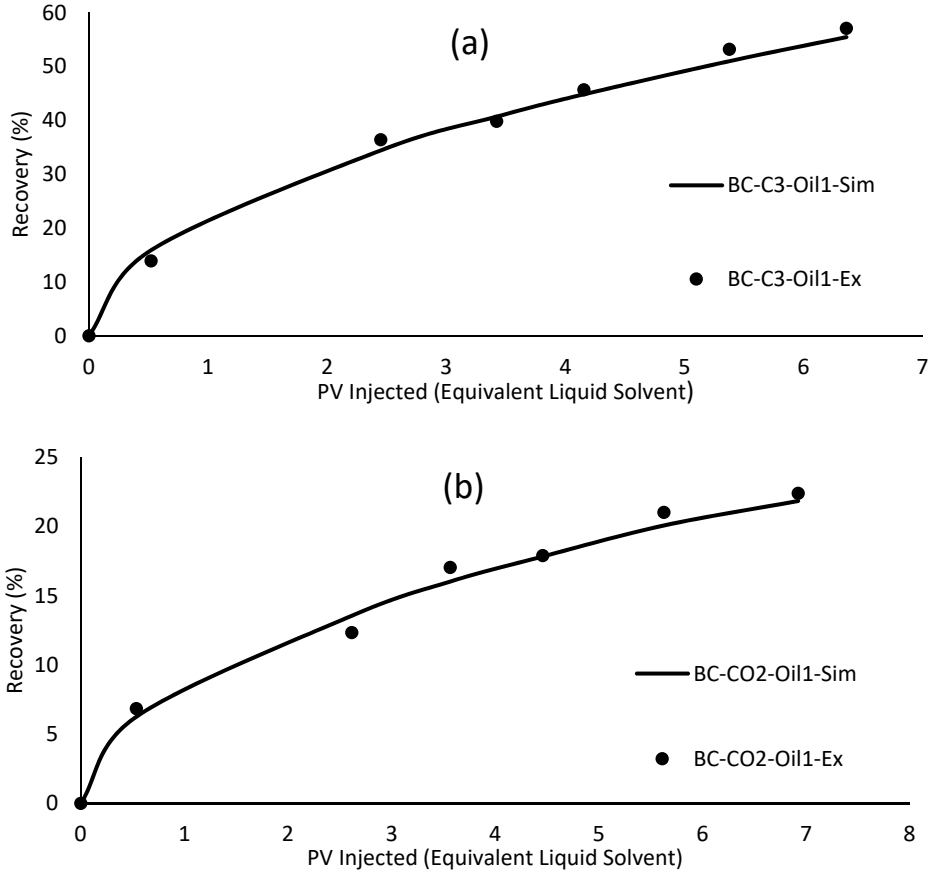

Figure 8. History matching results in the base case scenario with (**a**) C_3H_8, and (**b**) CO_2.

3. Results and Discussion

As mentioned in the experimental procedures, a total of 18 VAPEX experiments were carried out by employing various fracture patterns, a typical Canadian heavy oil sample,

and two gas solvents. The solvents included pure propane and pure carbon dioxide. All tests were conducted at room temperature, and, to comply with the constant pressure nature of VAPEX, the initial reservoir pressure and production (BPR) pressure were fixed at 790 kPa, while solvent injection occurred at 800 kPa. Table 2 summarizes the main operational information for each test. The effects of the main fracture parameters, including fractures' orientation, length, width, intensity, and position on process performance, were evaluated. The ultimate recovery factors with respect to the pore volumes of solvent injected, solvent types, and solvent–heavy oil ratio are discussed in this section.

Table 2. The designed VAPEX tests in the fractured reservoirs.

Test No.	Pattern	Solvent	Fracture Inclination	Fracture Length (mm)	Fracture Width (mm)	Fracture Intensity
1	Base case	CO_2	-	-	-	-
2	Base case	C_3H_8	-	-	-	-
3	H1	CO_2	Horizontal	34	2	2
4	H1	C_3H_8	Horizontal	34	2	2
5	H2	CO_2	Horizontal	34	2	2
6	H2	C_3H_8	Horizontal	34	2	2
7	H3	CO_2	Horizontal	34	2	3
8	H3	C_3H_8	Horizontal	34	2	3
9	H4	CO_2	Horizontal	51	2	2
10	H4	C_3H_8	Horizontal	51	2	2
11	H5	CO_2	Horizontal	34	2	2
12	H5	C_3H_8	Horizontal	34	2	2
13	H6	CO_2	Horizontal	34	4	2
14	H6	C_3H_8	Horizontal	34	4	2
15	V1	CO_2	Vertical	34	2	2
16	V1	C_3H_8	Vertical	34	2	2
17	V2	CO_2	Vertical	34	2	4
18	V2	C_3H_8	Vertical	34	2	4
19	V3	CO_2	Vertical	34	2	8
20	V3	C_3H_8	Vertical	34	2	8
21	V4	CO_2	Vertical	34	4	4
22	V4	C_3H_8	Vertical	34	4	4
23	V5	CO_2	Vertical	17	2	2
24	V5	C_3H_8	Vertical	17	2	2
25	V6	CO_2	Vertical	17	2	4
26	V6	C_3H_8	Vertical	17	2	4
27	V7	CO_2	Vertical	34	2	2
28	V7	C_3H_8	Vertical	34	2	2
29	V8	CO_2	Vertical	34	2	2
30	V8	C_3H_8	Vertical	34	2	2

3.1. Base Case Scenario

The pattern used in this VAPEX experiment includes no fractures and serves as a reference for the other fractured designs. Figure 9 demonstrates the recovery factors from

tests 1–2 with respect to the pore volume of the solvent injected. As can be seen, both the experimental and simulation outcomes appear on the plot. As expected, all graphs represent an increasing trend in their recovery values as the process proceeds, with propane yielding a considerably higher RF. One can attribute this significant disparity to the solvents' abilities in diffusing and dispersing into the bulk of heavy oil.

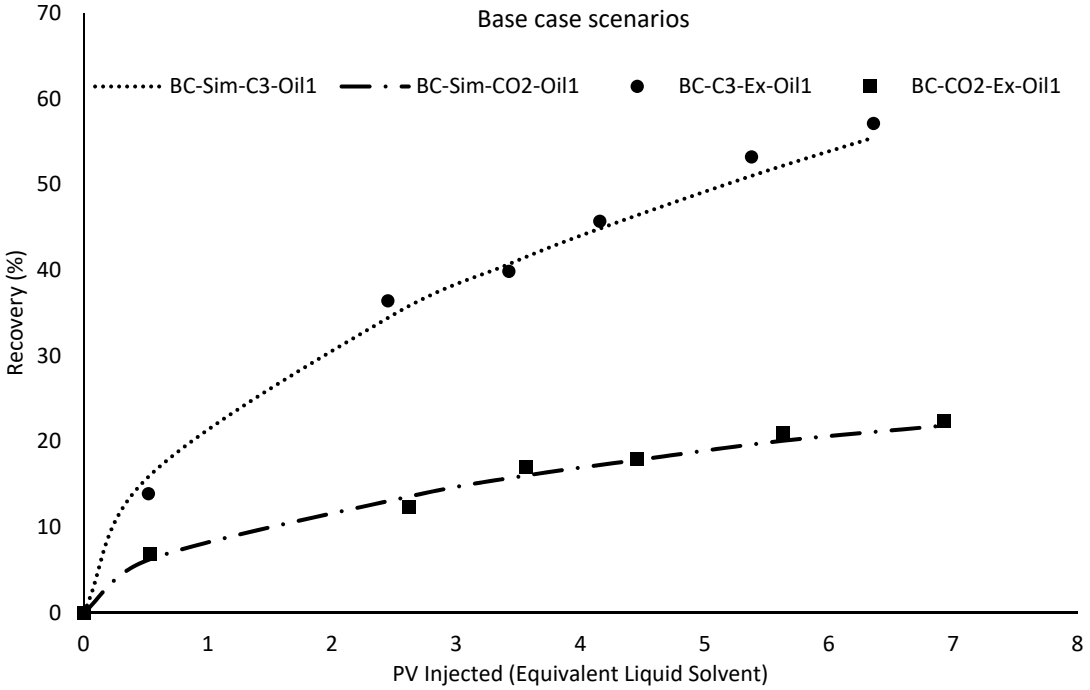

Figure 9. The base case scenario results for propane and carbon dioxide injection.

Furthermore, fluctuations in the heavy oil recovery data, as apparent among the experimental data, can be related to heavy oil re-imbibition in the swept zones, asphaltene precipitation in the vicinity of the production well, or experimental equipment, such as the back pressure regulator. Similar observations were reported by other researchers [35–37]. Remarkable agreement can be observed between the simulation and experimental results for both indicated scenarios.

When analyzing the impact of each fracture parameter, one may note that the conclusions made may change when changing other fracture parameters, such as their position. It is important to recognize that fractures that exist between injection and production wells can have a significant impact on breakthrough of solvents, the gravity drainage mechanism, and, ultimately, the recovery factor. When investigating the effect of a particular fracture parameter, attempts have been made to select the most relevant patterns to obtain precise evaluations and performance comparisons.

3.2. Effect of Fracture Orientation

Patterns H2 and V1 were selected to represent a horizontal and vertical fracture configuration and to be compared against the base case scenario. They were selected for the evaluations and comparisons due to the equal fracture lengths and similar positions near the injection well. As shown in Figure 10, the experimental outcomes and simulation results highlight that the presence of both fracture designs increases the recovery factor when using both solvent types.

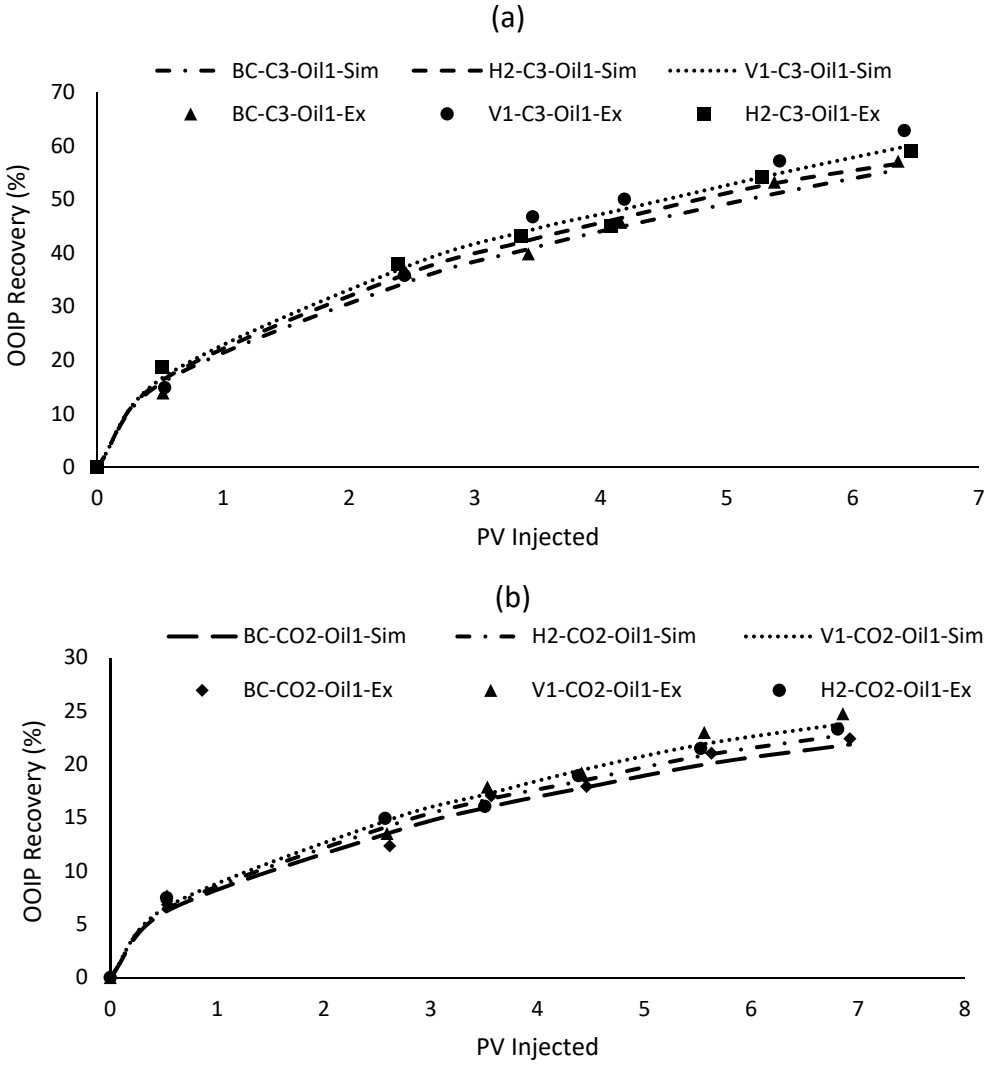

Figure 10. The effect of fracture orientation on the recovery factors in conventional VAPEX and patterns H2 and V1 using propane (**a**) and carbon dioxide (**b**).

When compared to the 57.12% RF obtained at the end of an experiment in a conventional VAPEX test using C_3H_8, patterns H2 and V1 led to 59.05% and 62.83%, respectively, under the same operational circumstances. The recovery factors reported by the simulator for the same three VAPEX tests show 55.48% and 59.79%, respectively, which are in complete agreement with the experimental results. The enhanced production in both cases of horizontal and vertical fractured patterns originates from the increased solvent–heavy oil contact in the presence of the fractures. Indeed, the fractures facilitate solvent access further into the bulk of the reservoir and, hence, enhance production and recovery.

Moreover, one may notice the higher RF recorded at the end of the VAPEX process when employing the vertical fracture configuration (V1) in comparison to the horizontal (H2). This can be attributed to creation of high-permeability flow paths for the solvent and heavy oil in the vertical direction into regions that would remain untouched otherwise. In other words, vertical fractures significantly enhance the vertical permeability of the heavy oil reservoir. Therefore, the mass transfer and gravity drainage mechanisms are considerably improved.

To mention another reason for witnessing greater process enhancement when employing vertical fracture configurations, one may allude to the fact that horizontal fractions facilitate solvent access in the same direction that the solvent chamber grows. Therefore,

some or all those areas, depending on the fractures' positions, might eventually be touched and swept by the injected solvents even in the absence of the horizontal fractures.

In addition, due to their horizontal direction, these fractures do not provide any means for improving the gravity drainage mechanism and, hence, do not happen to have as great of an impact on the RF as that by the vertical fractures. However, the overall impact depends on other parameters, such as position and the extension by which fractures penetrate the untouched zones.

A similar analysis after experimentally using CO_2 as the solvent reveals the performance of the conventional VAPEX was raised from an RF of 22.4% to 23.31% and 24.74% when carried out in H2 and V1 patterns, respectively. As per the simulation results for the same three VAPEX tests, 21.85% for the conventional case, 22.66% for H2, and 23.78% for V1 were found by the simulator. In accordance with the results of using C_3H_8, these data manifest a higher recovery factor after running VAPEX in both patterns, with V1 showing superior performance due to the reasons mentioned above. Similar trends and numbers can be found in case of solvent mixture injection.

3.3. Effect of Fracture Length

To investigate the effect of fracture length on the VAPEX process, horizontal patterns H1 and H4 and the two vertical sets of patterns, V1 and V5, as well as V2 and V6 were selected. Patterns H1 and H4 possess the same fracture width (2 mm), intensity (2 fractures per pattern), orientation (horizontal), and position (between the injection and production wells), while their only distinction lies in their length. The fracture lengths in the former and latter patterns are 34 and 51 mm, respectively. A similar statement can be made about fractures V1 and V5, as well as V2 and V6. Fractures V1 and V5 both possess a width of 2 mm and an intensity of two fractures per pattern, are vertically oriented, and are placed on either side of the injection/production well pair. However, the fractures in V1 are 34 mm long, while the ones in V5 are 17 mm long. Fractures V2 and V6 follow the same pattern as V1 and V5, respectively, with their only discrepancy being the fracture intensity of four per pattern (two on either side of the well pair).

As Figures 11–13 depict, all these patterns yield significantly higher recovery factors in comparison to the base case, as mentioned in the previous section. This is the case when using both solvents and is confirmed by both experimental and simulation outcomes. Using propane for the H1 pattern, the recorded experimental and simulation-based ultimate RF values are 64.22% and 61.41%, respectively, while, for H4, those factors are 68.41% and 64.93%, respectively. Therefore, it can be concluded that, with an increase in fracture length by a factor of 1.5, the RF is raised by 4.19% and 3.52% in total RF from experimental and simulation points of view, respectively. Conducting the VAPEX experiment in pattern H4 resulted in the highest ultimate RF obtained among the horizontal patterns, and almost the highest among all scenarios, primarily due to the extended fracture length, which facilitates solvent access to the far-fetched regions of the porous media. Moreover, the positioning of the fractures between the two well pairs further improves the gravity drainage mechanism, which, in turn, enhances recovery.

Furthermore, when using carbon dioxide in the same arrangements, an increase of 1.98% from 24.93% in H1 to 26.91% in H4 was recorded in the simulation-based results, while this number was 1.99% in the experimental results, where a recovery of 26.05% in H1 was raised to 28.04% in H4 due to the larger fracture length.

When using propane in patterns V1 and V5 saturated with heavy oil type 1, due to the fracture lengths being reduced to one-half in V5, the recorded simulation-based recovery factors were 59.79% and 57.2%, respectively. This shows a 2.59% decrease. The experimental RF for V1 was found to be 62.83%, while results from V5 were simulation-based only and, hence, no experimental data were available. One may notice that even the short fractures placed on either side of the injection/production well pair lead to a higher RF in comparison to the conventional VAPEX setting, which, for this case, was 55.48%. Furthermore, using CO_2 for the same heavy oil pattern systems, simulation-based

recovery factors were found to be 23.78% and 22.75%, respectively, which reveals a decrease in the RF of 1.03%. Finally, the experimental value obtained for V1 was 24.74%, which is in close agreement to its corresponding simulation outcome. Further scrutiny of the numbers obtained from mixture solvent injection yields similar trends.

Similar to the comparison made between V1 and V5, reducing the vertical fracture length in half from V2 to V6 led to a similar outcome. This time, the designed patterns included two vertical fractures on either side of the well pair and the obtained data were through simulation only. In the case of utilizing propane, the recovery factor dropped by 4.58% from 63.77% recorded in V2 to 59.19% in V6. This reduction was also observed when injecting CO2 into the same patterns, where a drop of 1.85% was observed. Running the VAPEX simulations in patterns V2 and V6 resulted in recoveries of 25.39% and 23.54%, respectively.

The improved recoveries among the three compared pattern pairs can be attributed to increased solvent–heavy oil contact. This effect is emphasized when access is provided to the harder-to-reach regions in the porous media. Furthermore, the gravity drainage mechanism is enhanced, even though not as effectively with the horizontal fractures as with the vertical ones. Finally, the existence of these fractures boosts the solvent chamber propagation, especially in fractures close to the injection well as the injected solvent can find an easy path to access the bulk of the heavy oil.

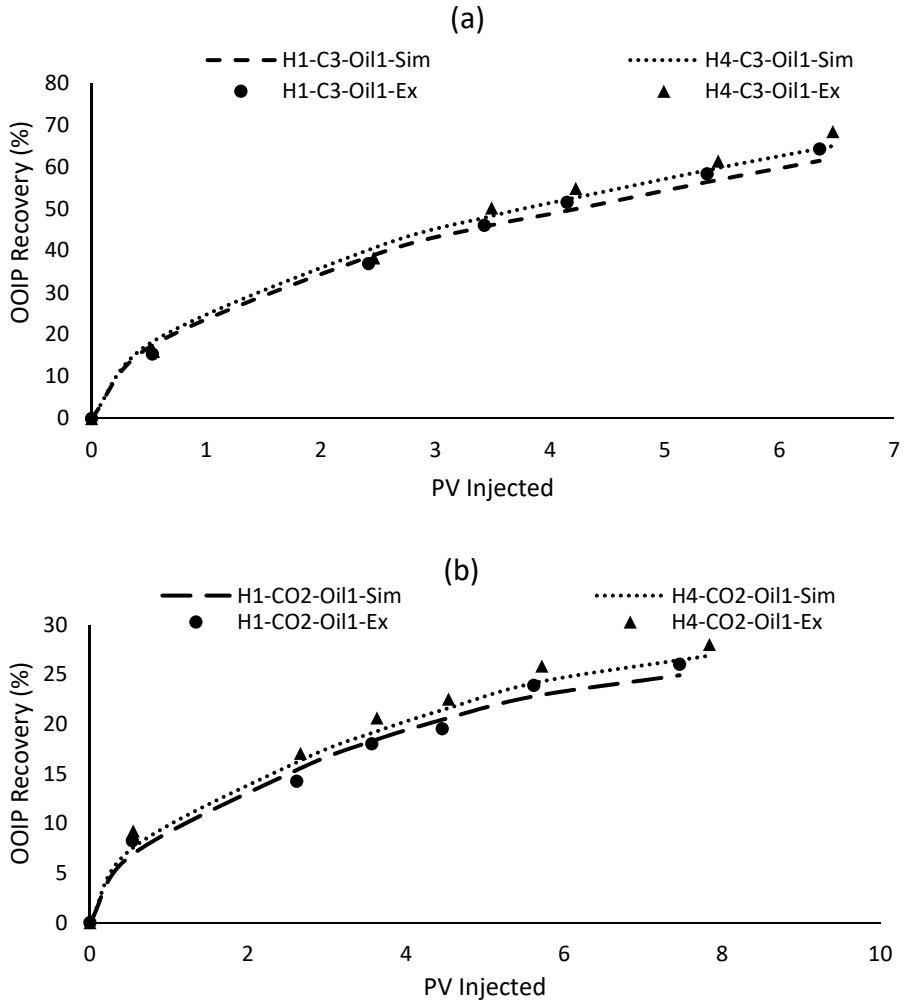

Figure 11. The effect of fracture length on the recovery factors in conventional VAPEX and patterns H1 and H4 using propane (**a**) and carbon dioxide (**b**).

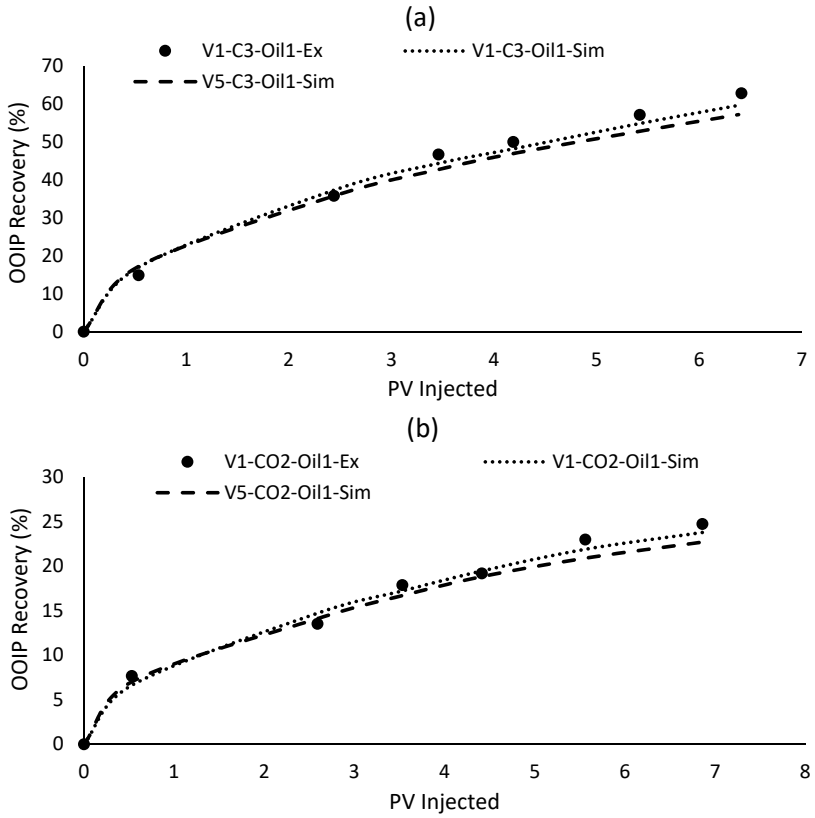

Figure 12. The effect of fracture length on the recovery factors in conventional VAPEX and patterns V1 and V5 using propane (**a**) and carbon dioxide (**b**).

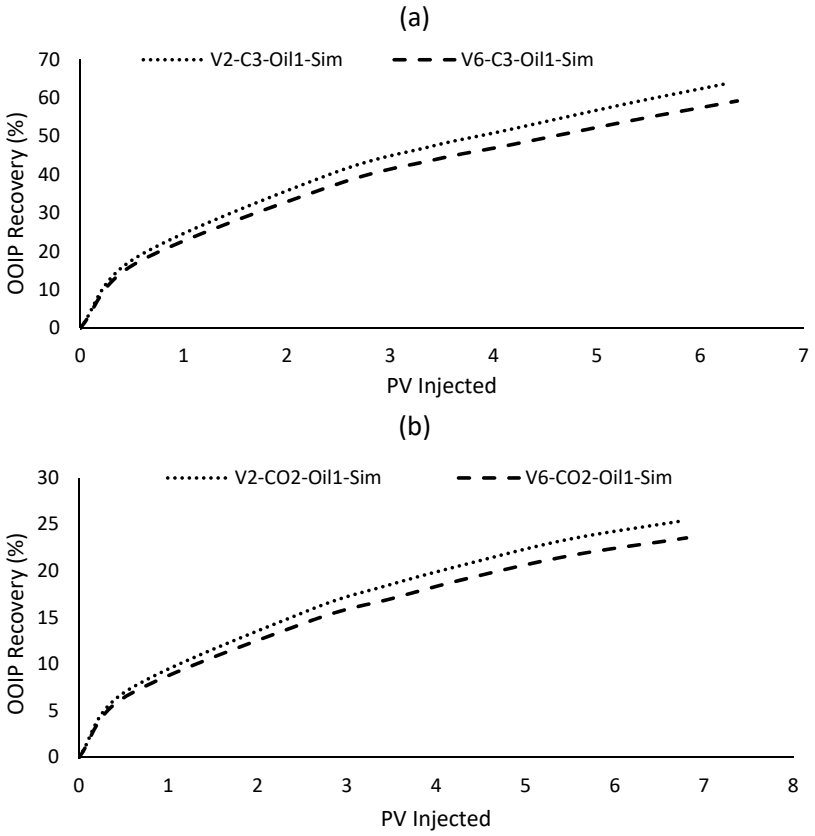

Figure 13. The effect of fracture length on the recovery factors in conventional VAPEX and patterns V2 and V6 using propane (**a**) and carbon dioxide (**b**).

3.4. Effect of Fracture Width

In this section, patterns H5 and H6 are selected for conducting recovery factor comparisons with the purpose of identifying the effect of fracture width on VAPEX performance in horizontal formations. Thereafter, patterns V2 and V4 undergo a similar comparison to further assess the same parameter for vertically fractured reservoirs. In both analyses, the fracture width is doubled while maintaining the rest of the process parameters. Due to the strong link between fracture width and permeability, the associated value for fracture permeability was doubled as well.

In patterns H5 and H6, the two horizontal fractures are located above and below the injection well while doubling the fracture width from an initial value of 2 mm to 4 mm from H5 to H6. The fractures' length (34 mm), intensity (2 per pattern), position, and inclination (horizontal) remain the same in the transition. The same can be said about V2 and V4, except for fracture intensity, which is four per pattern. Figures 14 and 15 demonstrate the obtained RF of these pattern pairs on the same plot.

As can be seen in Figure 14, doubling the fracture width in the horizontal patterns results in a slight increase of 1.67% in the recovery factor. This is simply due to the greater solvent access to the bulk of the heavy oil. A similar growth in total production is observed when employing carbon dioxide (0.98%). In addition, the experimental RFs at the end of the VAPEX test in the H6 pattern using propane and carbon dioxide were 61.92% and 24.75%, which are in agreement with the simulation-based outcomes.

Figure 15 represents the recovery factors obtained using vertically fractured patterns V2 and V4. The increased fracture width from V2 to V4 in both scenarios of using propane and carbon dioxide as the injection solvent leads to notable growth in the ultimate recovery factor. As can be seen, the RF is raised by 2.04% from a value of 63.77% in V2 to 65.81% in V4, which is confirmed by an experimentally obtained recovery of 68.30%.

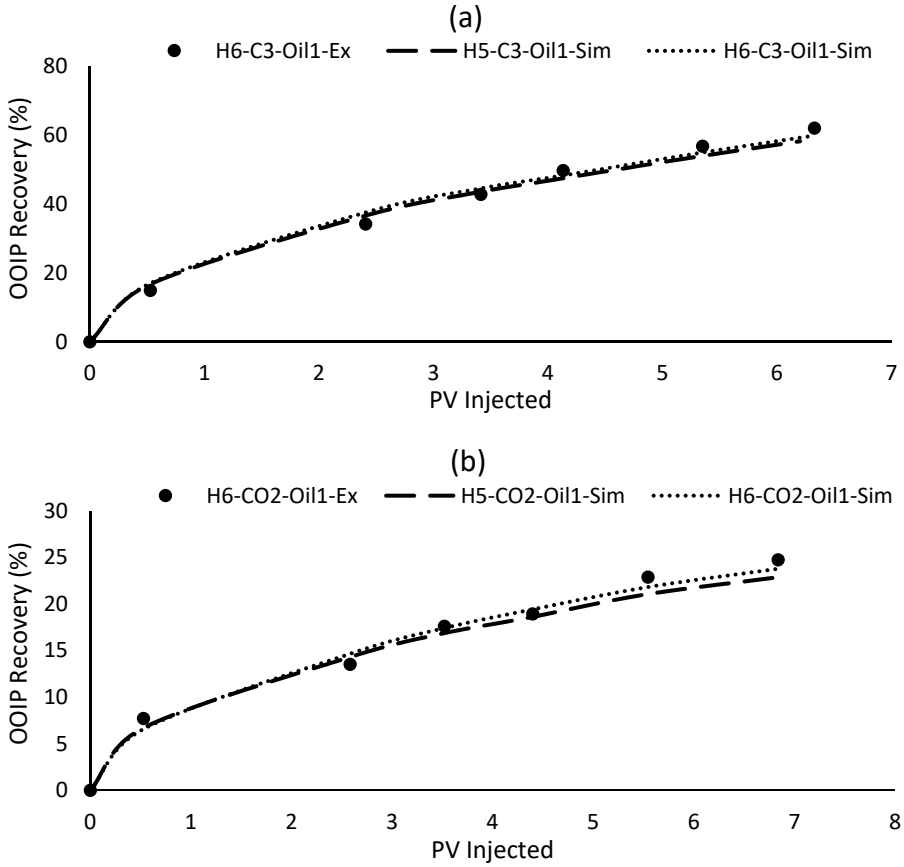

Figure 14. The effect of fracture width on the recovery factors in conventional VAPEX and patterns H5 and H6 using propane (**a**) and carbon dioxide (**b**).

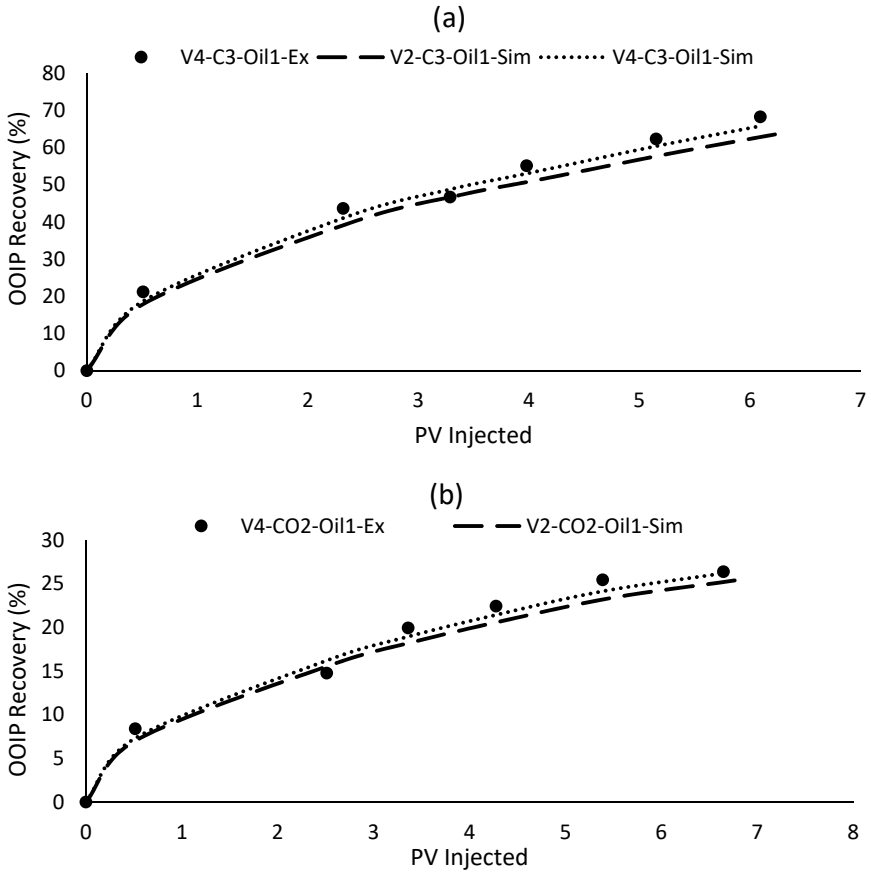

Figure 15. The effect of fracture width on the recovery factors in conventional VAPEX and patterns V2 and V4 using propane (**a**) and carbon dioxide (**b**).

It must be mentioned that this is the highest recovery factor recorded among all the designed patterns using both heavy oil types and the three injection solvents. In the case of injecting CO_2, also, an increase of 0.82% was observed as the recovery was observed to rise from 25.39% in V2 to 26.21% in V4. The experimental RF found in V4, 26.39%, confirms the simulation-based outcomes. The caused increase is less pronounced when using carbon dioxide due to the higher efficiency of propane in mixing with the heavy oil during the VAPEX process.

Overall, increasing the fracture width caused higher ultimate RF when employing both solvents in the two sets of comparisons made between H5 and H6, as well as V2 and V4. This is primarily due to the greater access to the heavy oil bulk provided by the widened fractures. However, unlike the case with fracture length, the difference between the extents to which this extra contact surface is provided is not overly significant. Hence, the difference between the process performance of H5 and H6 (increasing fractures' width) is not as large as the difference between H1 and H4 (increasing fractures' length) because the latter makes possible much larger reservoir contact.

3.5. Effect of Fracture Intensity

To study the effect of fracture intensity on the performance of the VAPEX process, patterns H2 and H3 were selected for recovery comparisons among the horizontally fractured models. Then, a similar results analysis was conducted for patterns V1, V2, and V3 to determine the same effect among the vertically fractured ones. The fracture intensity was increased from two to three from pattern H2 to H3, while the initial two fractures in V1 were doubled in V2, which was later doubled again to build V3. Other fracture parameters, such as length, width, orientation, and position, were kept the same in the series of simulations and experiments.

In both patterns H2 and H3, the fractures are positioned above the injection well to investigate their effect on spreading of the solvent chamber and, subsequently, the RF. Meanwhile, in V1, one fracture was designed on either side of the well pair (total of two). Then, another was added to each side (total of four) to create V2 and later experienced the same increase of fractures to four on each side (total of eight) to reach the design of V3. Figures 16 and 17 illustrate the VAPEX recovery factors in each of these patterns by using propane and carbon dioxide as the injection solvents.

Addition of another horizontal fracture above the injection well does not considerably enhance the heavy oil recovery factor. The recorded 57.01% (experimentally 59.05%) at the end of the VAPEX process using propane conducted in H2 grew to 57.56% due to inclusion of the third horizontal fracture in H3, marking an enhancement of only 0.55%. This can be related to the positioning of the fractures as the newly added one is not located between the injection/production well pair, where the gravity drainage is the most active and the diluted heavy oil moves down toward the production well. Hence, as already mentioned, when analyzing the simulation and experimental results, one may consider the fact that fracture parameters are influenced by each other and are not completely independent. For example, as will be shown in the next section, if, instead of adding a third horizontal fracture above the injection well to create H3 only one of the existing two was moved down to the space between the well pair (pattern H5), the recovery factor would be 58.11% (experimentally 60.24%). This shows that the RF will not increase just because of the existence of a higher number of fractures but rather depends on other crucial parameters, such as position with respect to the well pair. A compatible result was obtained when using carbon dioxide, where recovery was raised from 22.66% in H2 to 22.74% in H3, hence registering a growth of merely 0.08%.

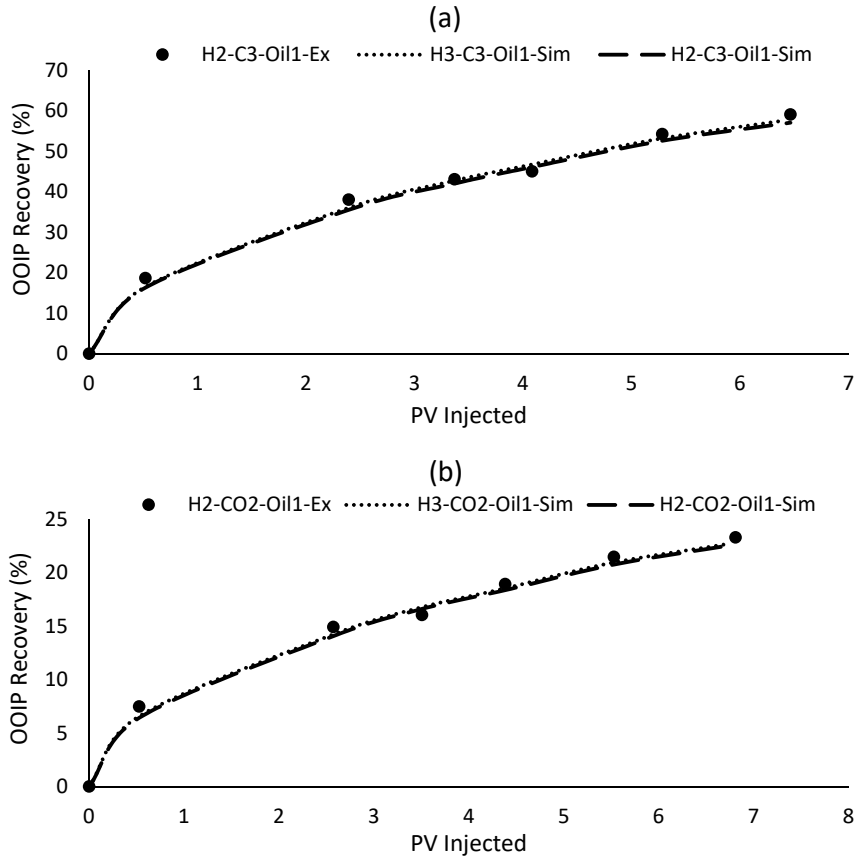

Figure 16. The effect of fracture intensity on the recovery factors in conventional VAPEX and patterns H2 and H3 using propane (**a**) and carbon dioxide (**b**).

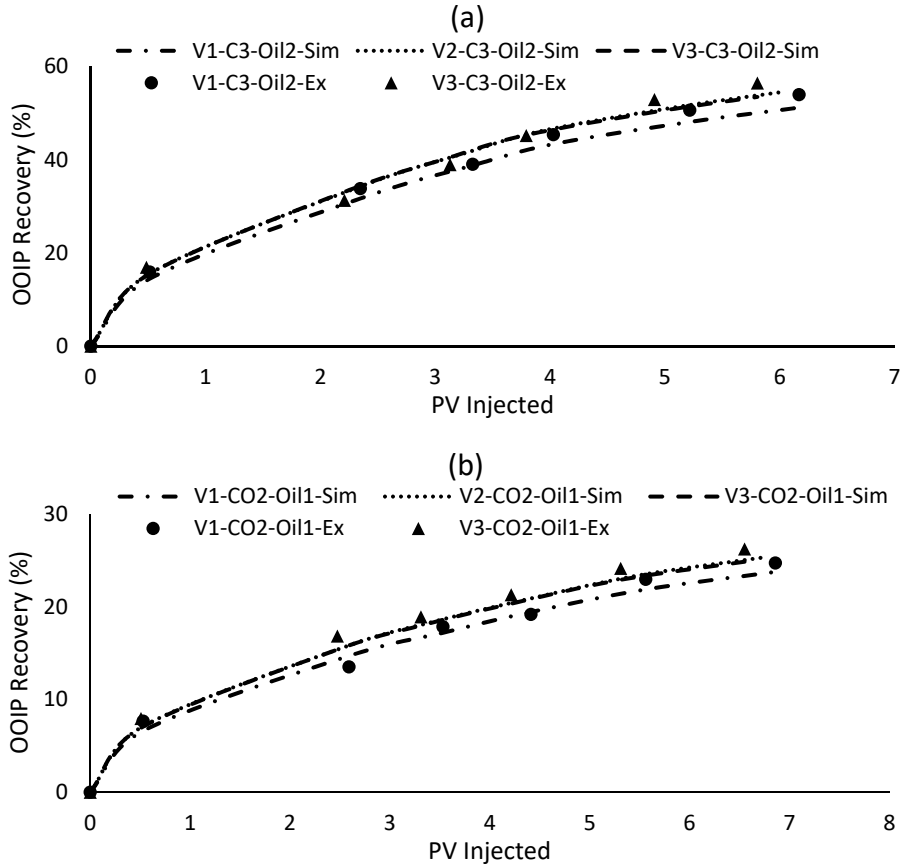

Figure 17. The effect of fracture intensity on the recovery factors in conventional VAPEX and patterns V1, V2, and V3 using propane (**a**) and carbon dioxide (**b**).

In the case of vertically fractured patterns, increasing fracture intensity from two to four (V1 to V2) per pattern caused remarkable RF growth of almost 4%. According to the simulation-based findings, conducting the VAPEX test using propane in pattern V1 resulted in production of 59.79% of the original oil in place, whereas the same test in V2 yielded 63.77%. The experimentally registered recovery factor for V1, 62.83%, is in good agreement with the simulation-based data, with an absolute error value of below 6%. However, the further increase brought about in the number of fractures to a total of eight in pattern V3 did not cause a recovery enhancement but a slight decrease in it with 62.38% in comparison to V2. Likewise, the RF decreased from 25.39% in V2 to 24.88% in V3 when utilizing carbon dioxide as the solvent.

This can be related to the high-permeability zone blockage phenomenon, which refers to trapping of the injected solvent in the numerous existing fractures and, hence, prevention from further mixing of the solvents with untouched zones. Therefore, the presence of an excessive number of vertical fractures, despite providing greater solvent–heavy oil contact, does not necessarily improve recovery while demanding even larger quantities of the injection solvent.

3.6. Effect of Fracture Position

This section focuses on studying the effect of fractures' positioning within the porous media on the efficiency of the VAPEX process. Patterns H1, H2, and H5 are used to compare the efficiency of horizontally fractured patterns, while V1, V7 and V8 serve the purpose of comparing VAPEX performances in vertically fractured formations.

Patterns H1 and H2 include two horizontal fractures below and above the injection well, respectively, while pattern H5 includes one fracture above the injector and another between the well pair. On the other hand, pattern V1 encompasses two vertical fractures

one on each side of the well pair. Then, patterns V7 and V8 include the same two fractures located farther away from the well pair halfway toward the reservoir boundaries and close to the reservoir boundary (farthest away from the well pair in the center of the pattern), respectively. The rest of the fracture parameters remain the same throughout these VAPEX tests. Figures 18 and 19 demonstrate the results obtained from simulation runs and experimental tests.

As depicted in Figure 18, in both cases of using propane and carbon dioxide, the ultimate recovery factor is noticeably higher when conducting VAPEX in pattern H1, which is followed by H5, leaving H2 as the one resulting in the lowest value among the three. This is corroborated by both simulation-based and experimental outcomes. The discrepancy in process performance can be attributed to placement of two horizontal fractures between the well pair, which, in addition to providing contact between the injected solvent and heavy oil, fortifies the gravity drainage mechanism. H2 provides the least contribution to the gravity drainage, while that of H5 can be assumed in between the two. The simulation-based and experimental RFs found for VAPEX in H1, H5, and H2 are 61.41% and 64.22%, 58.11% (only simulation-based data available for H5), and 57.01% and 59.05%, respectively (propane injection).

By comparing the simulation results, one may determine in increase of 1.1% in the recovery factor when one of the fractures is moved from above the injection well (H2) to the space between that and the production well (H5). Further growth of 3.3% is identified when moving the second fracture into the inter-well space (H1), hence registering a total increase of 4.4% between patterns H2 and H1. Analyzing the experimental findings leads to a similar enhancement of 5.17% when switching from H2 to H1.

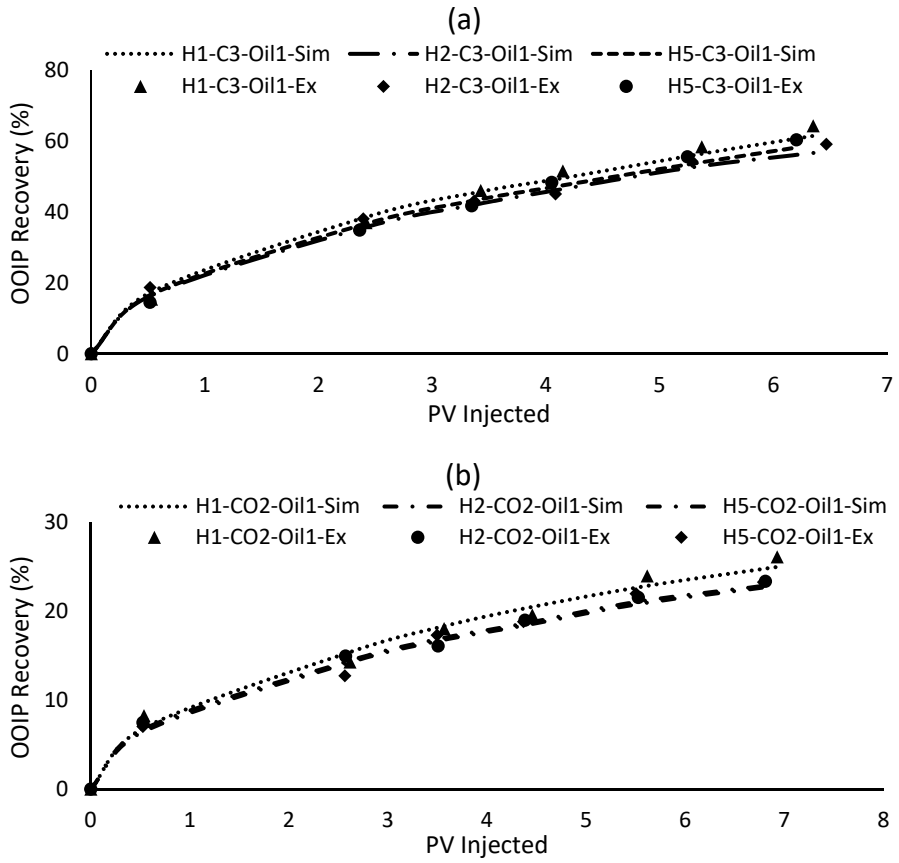

Figure 18. The effect of fracture position on the recovery factors in conventional VAPEX and patterns H1, H2, and H5 using propane (**a**) and carbon dioxide (**b**).

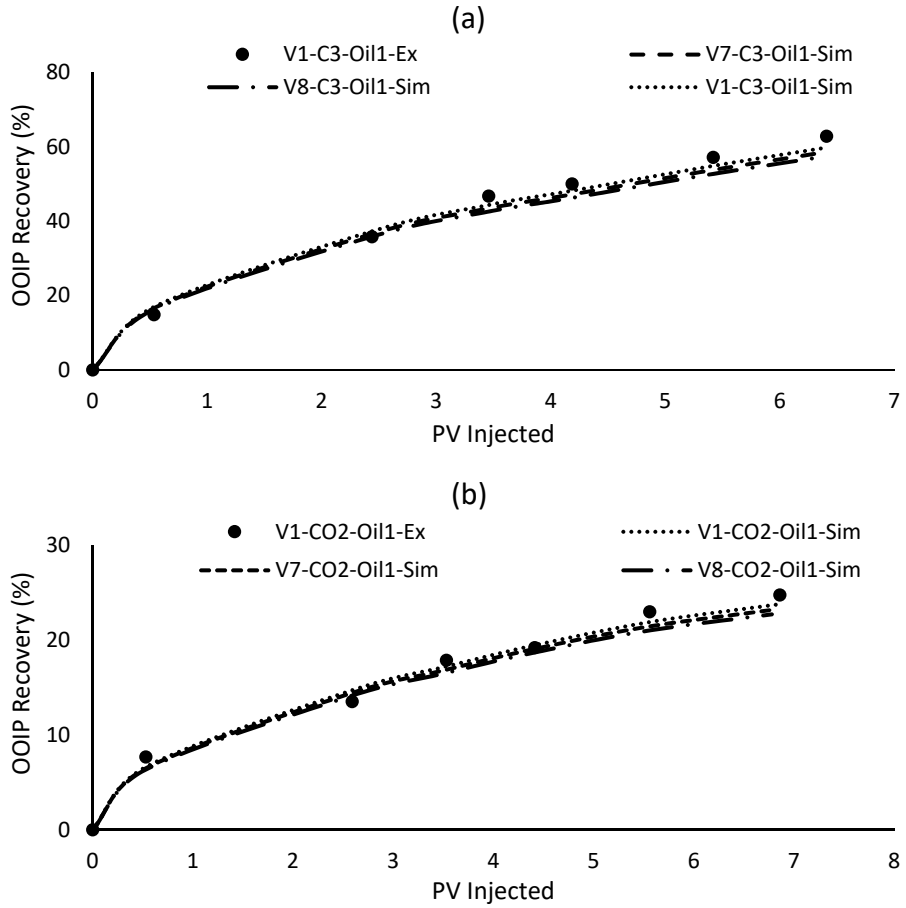

Figure 19. The effect of fracture position on the recovery factors in conventional VAPEX and patterns V1, V7, and V8 using propane (**a**) and carbon dioxide (**b**).

As indicated in Figure 18b, utilization of CO_2 causes a similar trend in the recovery factors. In H2, simulation-based and experimental outcomes of 22.66% and 23.31% were recorded, respectively. These numbers were increased to 24.93% and 26.05% in H1, respectively, highlighting enhancements of 2.27% and 2.74%. Meanwhile, the simulation-based recovery factor obtained after conducting VAPEX in H5 showed a value of 22.81%, which is reasonably less than that in H1 and higher than that in H2.

For the vertically fractured patterns, as the distance between the fractures and the well pair increases, the recovery factor decreases. As such, at the end of the VAPEX process using propane, the RF obtained in pattern V1 is the largest recorded, both experimentally and through simulation, with values of 62.83% and 59.79%, respectively. Simulation-based comparison with the other two cases reveals a reduction of 1.49% to reach 58.30% in V7 and of 2.69% to register 57.10% in V8. Similar reductions in the RF were noticed when carbon dioxide was the solvent used in the processes. From a simulation-based point of view, reductions in RF of 0.59% and 1.07% were found between V1 and V7 and V1 and V8, respectively. The experimentally determined RF of 24.74% is in good agreement with that yielded by the simulator, 23.78%.

The reason for the decline in heavy oil production can be the fact that, when the fractures are located near the injection production well pair, they can enhance solvent chamber propagation and the gravity drainage mechanism more efficiently. With the distance between the fractures and the well pair growing, it is not possible for these two crucial mechanisms to be improved before the solvent chamber physically reaches to the fractures. Hence, the fractures do not practically impose any influence on the VAPEX process performance before that occurs.

This effect is more obvious when comparing pattern designs V1 and V8. As can be seen in Figures 4–9, the vertical fractures are placed too close to the reservoir boundaries, and, therefore, the solvent chamber must already have reached the boundaries before any recovery mechanisms are enhanced. However, after this occurs, these fractures facilitate access to the untouchable regions in the reservoirs—regions that would not be touched otherwise even through other fracture designs—and improve the solvent–heavy oil contact area. Therefore, when comparing the RFs obtained from the base case and pattern V8, one can notice an increase of 1.62% and 0.86% when using propane and carbon dioxide, respectively.

The residuals versus order plot displays the residuals in the order that the data were.

3.7. Solvent–Oil Ratios

During the VAPEX experiments and simulation runs, the volume of the solvents injected was recorded by using the DFMs and the simulator. Hence, the solvent–heavy oil ratio (SOR) could be obtained at any time by finding the ratio of the equivalent liquid solvent injected over the volume of the heavy oil produced. It must be mentioned that, during prior history matching of the simulator with the experimental results, the solvent injection volumes were checked and in close agreement with the data collected in the lab.

The patterns with the highest (V4) and lowest (base case) recovery factors result in the lowest and highest SORs for all cases of solvent injection. As the ultimate recovery factor decreases from pattern V4 to the other patterns, the SOR increases. This indicates more efficient solvent usage in the patterns that yield higher recovery factors. In other words, the fracture structures in such patterns facilitate more effective solvent–heavy oil interaction by increasing contact area and enabling more in-depth reservoir access for solvents.

In general, propane had greater success in keeping the SOR values lower. Depending on the heavy oil type used, these figures range from 1.02 to 1.37. On the other hand, injecting carbon dioxide, as shown in the tables, renders significantly larger SOR values, which begin from almost 3 and rise as high as 4.35. Such a remarkable discrepancy can be attributed to the solvents' abilities to diffuse in and effectively disperse the heavy oil toward the production well.

Finally, it can be claimed that the vertical fracture structures result in general in higher recovery factors and lower SORs. In all cases presented, three out of the top four VAPEX performances are obtained in the vertically fractured reservoirs, while pattern V4 proves to yield the highest RF and the lowest SOR among all patterns.

3.8. Pore-Scale Analysis

To further benefit from the clearcut visualization provided by the microfluidic models, a pore-scale investigation of heavy oil–solvent interactions was carried out in different regions within the model. Hence, in-depth analyses of different solvents and heavy oils interaction, sweep efficiencies, and residual oil saturations near the reservoir boundaries as well as higher- and lower-permeability regions were obtained. This also made possible comparisons between solvents' performances while showing the influence of fractures in solvent chamber growth in the VAPEX tests.

Figure 20 depicts the difference between employing propane and carbon dioxide in the same pattern. As can be observed, the magnified parts of the images show the same grains in the same pattern in two identical VAPEX tests, with the only distinction being the type of solvent injected. Accordingly, using propane, due to its significantly higher diffusion and effective dispersion, yielded higher sweep efficiency, leaving a lower quantity of heavy oil behind. Furthermore, the overall color of the system appears brighter when injecting propane, which implies a greater solvent–heavy oil interaction. Propane demonstrates greater capability in sweeping smaller pores (harder-to-reach zones) in comparison to the other two injected solvents.

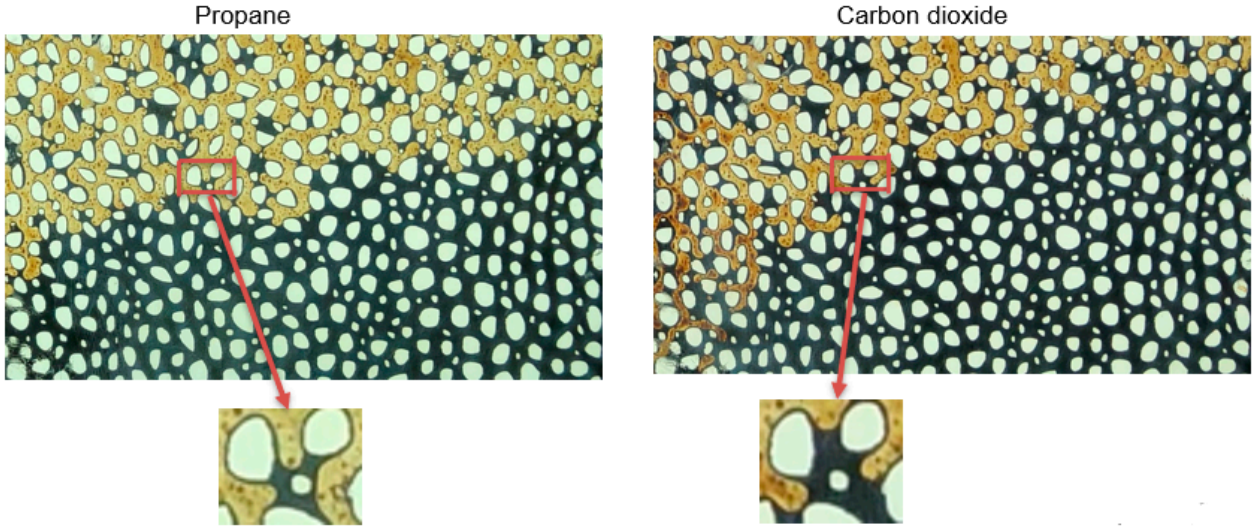

Figure 20. Solvent performance comparison between propane and carbon dioxide in the same reservoir pattern.

Figure 21 shows two VAPEX processes carried out in the conventional and fractured reservoirs. As depicted, existence of horizontal fractures led to formation of a lighter-color and more laterally spread solvent chamber, leaving less residual oil saturation behind. The images are captured at the same time in the experimental process to enable fair performance comparison.

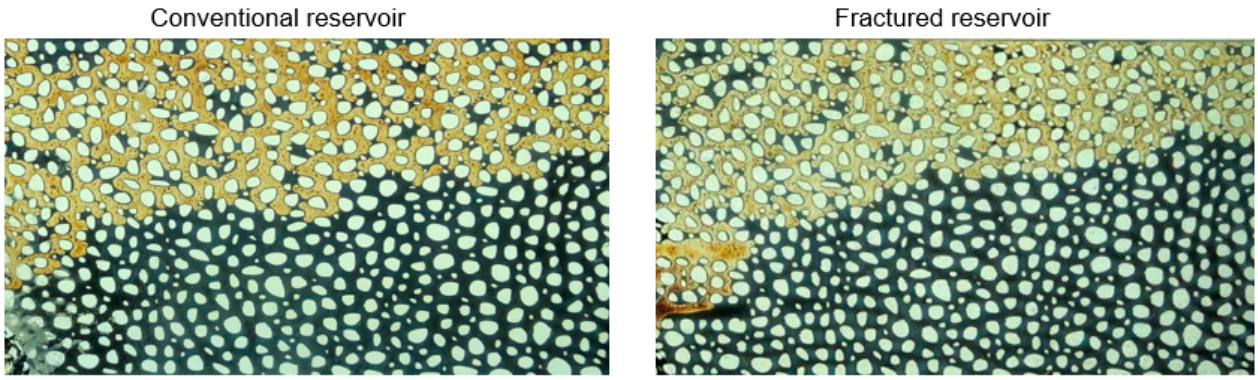

Figure 21. The VAPEX processes in the conventional and fractured reservoirs.

Finally, Figure 22 illustrates the solvent–heavy oil interactions near the reservoir top boundary. As indicated, injection of pure carbon dioxide results in significantly higher residual oil saturation in that region, while pure propane represents considerably greater ability in sweeping near-boundary areas. When the solvent mixture is introduced to the system, as expected, the sweep efficiency falls between that of the mentioned two, while, due to propane's significant diffusion and effective dispersion, it proves to be close to that observed in pure propane injection.

One may note that the microfluidic models utilized in this study were intended to be in relevant dimensions to fulfill use of such devices. Trial and error processes were carried out to determine optimum model sizes. Moreover, the two solvents employed mark the two bound values as propane is known as one of the most effective solvents (yet too expensive) and carbon dioxide alone renders minimum recovery factors. In other words, these solvents can be deemed to yield a low-to-high range of RFs in the VAPEX process.

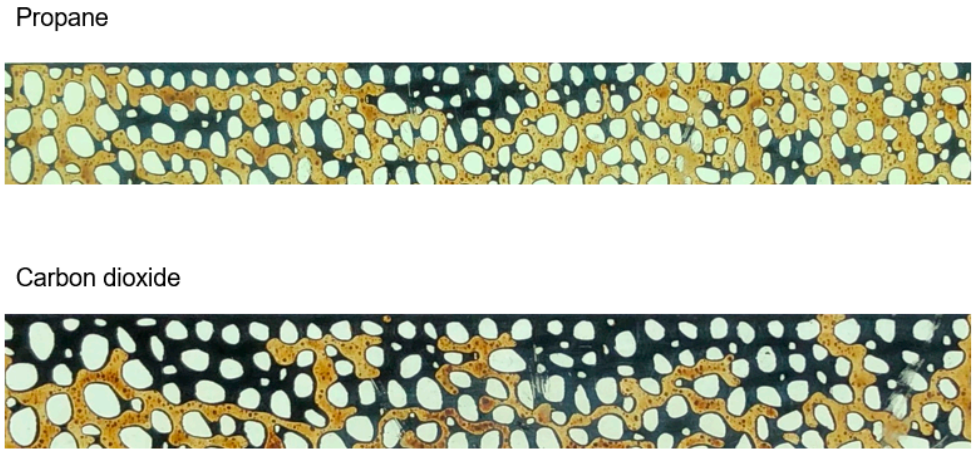

Figure 22. The solvent–heavy oil interactions near the reservoir top boundaries.

4. Conclusions

An extensive numerical and experimental investigation of fracture parameters' impact on VAPEX process performance was carried out utilizing state-of-the-art micromodels. Several fracture structures were designed and implemented on the reservoir patterns that were later saturated with two heavy oil samples. Propane demonstrated significantly higher efficiency in heavy oil recovery enhancement in comparison to carbon dioxide. This was mainly due to its significantly higher diffusion and dispersion, both of which combine as effective dispersion.

The highest ultimate recovery factor was achieved when injecting propane to a reservoir containing two long, wide vertical fractures on either side of the injection production well pair (pattern V4) saturated with heavy oil type 1. This was attributed to remarkably improved solvent–heavy oil contact area as well as the main VAPEX production mechanism, gravity drainage.

The lowest ultimate recovery factor was obtained when injecting carbon dioxide to the conventional reservoir (not fractured).

According to the image analyses performed regarding both heavy oil–solvent systems, vertical fractures brought about more significant heavy oil recovery enhancements in comparison to the horizontal fractures. This is mainly due to improvement in the main production mechanism in the VAPEX process—gravity drainage. Furthermore, vertical fractures allow the solvent access to regions that are otherwise harder to reach, especially when these fractures are located farther away from the well pair.

The fracture parameters impact each other's efficiency, and, therefore, all of them must be considered when drawing conclusions. For example, fracture positioning can impose significant changes on the influence of other parameters on the VAPEX process. In both vertically and horizontally fractured reservoirs, increasing fracture length caused remarkable increases in the recovery factor. While this happened for both solvents, it was more sensed with propane injection.

Increasing the fracture width resulted in recovery enhancements due to providing a larger solvent–heavy oil contact area. However, the extent to which contact area is increased is not as large as that regarding fracture length increase; therefore, the enhancement observed in the ultimate recovery factor was not as large as that case.

By increasing the fracture intensity, the heavy oil recovery factor increased, but, after some point, it showed an adverse effect on process performance. This was observed when the number of vertical fractures was raised from four (two on each side of the well pair) to eight (four on each side of the well pair). This was due to the phenomenon known as high-permeability zone blockage. As a result of this phenomenon, an injected solvent fails to effectively diffuse and disperse in heavy oil due to being trapped in fractures; hence, it cannot be replaced by the newly injected solvent. Fracture position is one of the most important parameters that can also influence other parameters. The VAPEX test

outcomes revealed that horizontal fractures located between the well pair enhance the gravity drainage mechanism and boost process efficiency. Horizontal fractures placed above the injector did not significantly improve solvent chamber growth or solvent–heavy oil contact. Moreover, by placing the vertical fractures farther away from the centralized well pair and toward the reservoir boundaries, their effectiveness started to decline.

Author Contributions: Conceptualization, A.R.; methodology, A.R. and F.T.; software, A.R.; experiments, A.R.; formal analysis, A.R.; investigation, A.R. and F.T.; writing—original draft preparation, A.R.; writing—review and editing, A.R.; supervision, F.T. All authors have read and agreed to the published version of the manuscript.

Funding: This research received no external funding.

Data Availability Statement: The data used to support the findings of this study are available from the corresponding author upon request.

Conflicts of Interest: The authors declare no conflict of interest.

References

1. James, L.; Rezaei, N.; Chatzis, I. Vapex, Warm Vapex and Hybrid Vapex-the State of Enhanced Oil Recovery for in Situ Heavy Oils in Canada. *J. Can. Pet. Technol.* **2008**, *47*. [CrossRef]
2. Das, S.; Butler, R. Extraction of Heavy Oil and Bitumen Using Solvents at Reservoir Pressure. In Proceedings of the Technical Meeting/Petroleum Conference of the South Saskatchewan Section, Regina, SK, Canada, 15–17 October 1995.
3. Das, S.K. Vapex: An Efficient Process for the Recovery of Heavy Oil and Bitumen. *SPE J.* **1998**, *3*, 232–237. [CrossRef]
4. Singhal, A.; Das, S.; Leggitt, S.; Kasraie, M.; Ito, Y. Screening of Reservoirs for Exploitation by Application of Steam Assisted Gravity Drainage/Vapex Processes. In Proceedings of the International Conference on Horizontal Well Technology, Calgary, AB, Canada, 18–20 November 1996.
5. Lin, L.; Ma, H.; Zeng, F.; Gu, Y. A Critical Review of the Solvent-Based Heavy Oil Recovery Methods. In Proceedings of the SPE Heavy Oil Conference-Canada, Calgary, AB, Canada, 10–12 June 2014.
6. Banerjee, D.K. *Oil Sands, Heavy Oil & Bitumen: From Recovery to Refinery*; PennWell Books: Tulsa, OK, USA, 2012.
7. Upreti, S.; Lohi, A.; Kapadia, R.; El-Haj, R. Vapor Extraction of Heavy Oil and Bitumen: A Review. *Energy Fuels* **2007**, *21*, 1562–1574. [CrossRef]
8. Butler, R.; Jiang, Q. Improved Recovery of Heavy Oil by Vapex with Widely Spaced Horizontal Injectors and Producers. *J. Can. Pet. Technol.* **2000**, *39*. [CrossRef]
9. Kok, M.; Yildirim, Y.; Akin, S. Application of Vapor Extraction (Vapex) Process on Carbonate Reservoirs. *Energy Sources Part A Recovery Util. Environ. Eff.* **2009**, *31*, 377–386. [CrossRef]
10. Yildirim, Y. Application of Vapex (Vapour Extraction) Process on Carbonate Reservoirs. Master's Thesis, Middle East Technical University, Ankara, Turkey, 2003.
11. Dunn, S.; Nenniger, E.; Rajan, V. A Study of Bitumen Recovery by Gravity Drainage Using Low Temperature Soluble Gas Injection. *Can. J. Chem. Eng.* **1989**, *67*, 978–991. [CrossRef]
12. Frauenfeld, T.; Deng, X.; Jossy, C. Economic Analysis of Thermal Solvent Processes. In Proceedings of the Canadian International Petroleum Conference, Calgary, AB, Canada, 13–15 June 2006.
13. Torabi, F.; Jamaloei, B.Y.; Stengler, B.M.; Jackson, D.E. The Evaluation of Co 2-Based Vapour Extraction (Vapex) Process for Heavy-Oil Recovery. *J. Pet. Explor. Prod. Technol.* **2012**, *2*, 93–105. [CrossRef]
14. Gao, Q.; Dong, P.; Liu, C. Modeling and Simulation of Shale Fracture Attitude. *ACS Omega* **2021**, *6*, 7312–7333. [CrossRef]
15. Li, Q.; Wang, F.; Forson, K.; Zhang, J.; Zhang, C.; Chen, J.; Xu, N.; Wang, Y. Affecting Analysis of the Rheological Characteristic and Reservoir Damage of CO_2 Fracturing Fluid in Low Permeability Shale Reservoir. *Environ. Sci. Pollut. Res.* **2022**, *29*, 37815–37826. [CrossRef]
16. Li, Q.; Wu, J. Factors Affecting the Lower Limit of the Safe Mud Weight Window for Drilling Operation in Hydrate-Bearing Sediments in the Northern South China Sea. *Geomech. Geophys. Geo-Energy Geo-Resour.* **2022**, *8*, 82. [CrossRef]
17. Chen, Y.; Wang, S.; Shao, B.; Yuan, Z.; Xie, L.; Fan, J. Simulations on Flow Behaviors of Heavy Oil and Its Asphaltic Residues through Horizontal Pipe Using a Filtered Two-Fluid Model. *J. Pet. Sci. Eng.* **2022**, *208*, 109395. [CrossRef]
18. Renner, T. Measurement and Correlation of Diffusion Coefficients for CO_2 and Rich-Gas Applications. *SPE Reserv. Eng.* **1988**, *3*, 517–523. [CrossRef]
19. Schmidt, T.; Leshchyshyn, T.; Puttagunta, V. Diffusivity of CO_2 into Reservoir Fluids. In Proceedings of the 33rd Annual Technical Meeting of the Petroleum Society of CIM, Calgary, AB, Canada, 5–8 June 1982.
20. Pourabdollah, K.; Mokhtari, B. The Vapex Process, from Beginning up to Date. *Fuel* **2013**, *107*, 1–33. [CrossRef]
21. Kapadia, R.A.; Upreti, S.R.; Lohi, A.; Chatzis, I. Determination of Gas Dispersion in Vapor Extraction of Heavy Oil and Bitumen. *J. Pet. Sci. Eng.* **2006**, *51*, 214–222. [CrossRef]

22. El-Haj, R.; Lohi, A.; Upreti, S. Experimental Determination of Butane Dispersion in Vapor Extraction of Heavy Oil and Bitumen. *J. Pet. Sci. Eng.* **2009**, *67*, 41–47. [CrossRef]
23. Boustani, A.; Maini, B. The Role of Diffusion and Convective Dispersion in Vapour Extraction Process. *J. Can. Pet. Technol.* **2001**, *40*. [CrossRef]
24. Oduntan, A.; Chatzis, I.; Smith, J.; Lohi, A. *Heavy Oil Recovery Using Vapex Process: Scale-up Issues*; University of Waterloo: Waterloo, ON, Canada, 2001.
25. Yazdani, A.; Maini, B.B. Effect of Height and Grain Size on the Production Rates in the Vapex Process: Experimental Study. *SPE Reserv. Eval. Eng.* **2005**, *8*, 205–213. [CrossRef]
26. Butler, R.; Mokrys, I. Solvent Analog Model of Steam-Assisted Gravity Drainage. *AOSTRA J. Res.* **1989**, *5*, 17–32.
27. Moghadam, S.; Nobakht, M.; Gu, Y. Theoretical and Physical Modeling of a Solvent Vapour Extraction (Vapex) Process for Heavy Oil Recovery. *J. Pet. Sci. Eng.* **2009**, *65*, 93–104. [CrossRef]
28. Ma, H.; Yu, G.; She, Y.; Gu, Y. A Parabolic Solvent Chamber Model for Simulating the Solvent Vapor Extraction (Vapex) Heavy Oil Recovery Process. *J. Pet. Sci. Eng.* **2017**, *149*, 465–475. [CrossRef]
29. Pendar, H.; Salehi, M.M.; Kharrat, R.; Zarezadeh, S. Numerical and Anfis Modeling of the Effect of Fracture Parameters on the Performance of Vapex Process. *J. Pet. Sci. Eng.* **2016**, *143*, 128–140. [CrossRef]
30. Azin, R.; Kharrat, R.; Ghotbi, C.; Rostami, B.; Vossoughi, S. Simulation Study of the Vapex Process in Fractured Heavy Oil System at Reservoir Conditions. *J. Pet. Sci. Eng.* **2008**, *60*, 51–66. [CrossRef]
31. Azin, R.; Kharrat, R.; Ghotbi, C.; Vossoughi, S. Applicability of the Vapex Process to Iranian Heavy Oil Reservoirs. In Proceedings of the SPE Middle East Oil and Gas Show and Conference, Manama, Bahrain, 12–15 March 2005.
32. Azin, R.; Kharrat, R.; Ghotbi, C.; Vossoughi, S. Improved Heavy Oil Recovery by Vapex Process in the Presence of Vertical and Horizontal Fractures. *J. Jpn. Pet. Inst.* **2007**, *50*, 340–348. [CrossRef]
33. Marzbanfard, E.; Kharrat, R.; Azin, R. Experimental Study of Vapor Extraction (Vapex) in Fractured Reservoirs. In Proceedings of the 10th International Chemical Engineering Congress & Exhibition (IChEC), Isfahan, Iran, 6–9 May 2018.
34. Rostami, B.; Azin, R.; Kharrat, R. Investigation of the Vapex Process in High Pressure Fractured Heavy Oil Reservoirs. In Proceedings of the SPE International Thermal Operations and Heavy Oil Symposium, Calgary, AB, Canada, 1–3 November 2005.
35. Ahmadloo, F. Investigation of Interplay of Capillarity, Drainage Height, and Aqueous Phase Saturation on Mass Transfer Phenomena in Heavy Oil Recovery by Vapex Process. Ph.D. Thesis, The University of Regina (Canada), Regina, SK, Canada, 2012.
36. Jafarinazhad, A.Y. Physical and Numerical Modeling of Permeability and Drainage Height Effects in Vapex. Ph.D. Thesis, University of Calgary, Calgary, AB, Canada, 2007.
37. Mohammadpoor, M. Experimental, Numerical, and Soft Computing-Based Analysis of the Vapex Process in Heavy Oil Systems. Ph.D. Thesis, Faculty of Graduate Studies and Research, University of Regina, Regina, SK, Canada, 2014.